



Observed characteristics of dust storm events over the western United States using meteorological, satellite, and air quality measurements

H. Lei and J. X. L. Wang

National Oceanic and Atmospheric Administration (NOAA), Air Resource Laboratory, College Park, Maryland, USA

Correspondence to: J. X. L. Wang (julian.wang@noaa.gov) and H. Lei (hang.lei@noaa.gov)

Received: 8 April 2013 – Published in Atmos. Chem. Phys. Discuss.: 30 May 2013

Revised: 29 April 2014 – Accepted: 25 June 2014 – Published: 7 August 2014

Abstract. To improve dust storm identification over the western United States, historical dust events measured by air quality and satellite observations are analyzed based on their characteristics in data sets of regular meteorology, satellite-based aerosol optical depth (AOD), and air quality measurements. Based on the prevailing weather conditions associated with dust emission, dust storm events are classified into the following four typical types:

- (1) The key feature of cold front-induced dust storms is their rapid process with strong dust emissions.
- (2) Events caused by meso- to small-scale weather systems have the highest levels of emissions.
- (3) Dust storms caused by tropical disturbances show a stronger air concentration of dust and last longer than those in (1) and (2).
- (4) Dust storms triggered by cyclogenesis last the longest.

In this paper, sample events of each type are selected and examined to explore characteristics observed from in situ and remote-sensing measurements. These characteristics include the lasting period, surface wind speeds, areas affected, average loading on ground-based optical and/or air quality measurements, peak loading on ground-based optical and/or air quality measurements, and loading on satellite-based aerosol optical depth. Based on these analyses, we compare the characteristics of the same dust events captured in different data sets in order to define the dust identification criteria. The analyses show that the variability in mass concentrations captured by in situ measurements is consistent with the variability in AOD from stationary and satellite observations. Our

analyses also find that different data sets are capable of identifying certain common characteristics, while each data set also provides specific information about a dust storm event. For example, the meteorological data are good at identifying the lasting period and area impacted by a dust event; the ground-based air quality and optical measurements can capture the peak strength well; aerosol optical depth (AOD) from satellite data sets allows us to better identify dust-storm-affected areas and the spatial extent of dust. The current study also indicates that the combination of in situ and satellite observations is a better method to fill gaps in dust storm recordings.

1 Introduction

The western United States is an important source of global mineral dust emissions (Woodward, 2001; Tanaka and Chiba, 2006). Dust storms have seriously affected the western US and beyond in recent decades. Detailed reports on historical events trace back to the 1930s (Schubert et al., 2004). Main observing networks over the western US have included or collected airborne dust in their records or samples. For example, near-surface dust has been quantitatively sampled and tested for total aerosol mass concentrations by the Interagency Monitoring of Protected Visual Environments (IMPROVE) network and the US Environmental Protection Agency (EPA) Air Quality System (AQS). Similarly, the optical properties of dust weather events are recorded in aerosol optical depth (AOD) measurements by the Aerosol Robotic Network (AERONET) (Holben et al., 1998). In

addition, a number of spaceborne instruments have been used in satellites to capture optical depth, such as the Moderate Resolution Imaging Spectroradiometer (MODIS) (Remer et al., 2005), Multi-angle Imaging Spectroradiometer (MISR) (Kahn et al., 2009), and Total Ozone Mapping Spectrometer (TOMS) (Torres et al., 2002). Although dust has been recorded by a variety of observational systems, it is still difficult to quantify dust events because other aerosols (those produced by wildfire, industrial emissions, etc.) that have similar physical properties are also sampled or recorded together in the same measurements. As a result, complete or consistent dust event records are unavailable to the public or the scientific community.

As an extreme event, a dust storm is a major natural disaster that has affected both social life and public health in recent decades (Prospero, 1999; Tong et al., 2012). In the long term, frequent dust storms can affect climate, in addition to air quality and human health (Zhao et al., 2012). The media have reported some serious property losses for people in the western US due to dust storms in the past decade. The National Aeronautics and Space Administration's (NASA) earth observatory also captured some dust storm processes over the western US which affected areas of thousands of acres. Similarly, the anthropogenic dust events which are usually caused by ground vehicles, field constructions, industrial emissions, and agricultural activities also affect daily life. However, compared with them, dust storm events featuring high dust concentration levels are relatively easy to identify from measurements.

Indeed, a series of studies using different observations has been done to examine the particular characteristics of dust storms (Prasad and Singh et al., 2007; Hahnenberger and Nicoll, 2012). For instance, the characteristics of dust storm events have previously been examined using stationary aerosol concentration data from the IMPROVE network (Bell et al., 2007; Tong et al., 2012). The optical properties of dust storm events have also been analyzed based on laser detection in AERONET (Chin et al., 2009; Kim et al., 2011). Further, satellite data from MODIS and MISR have been used to retrieve the AOD measurements of dust storm events (Baddock et al., 2009; Waggoner and Sokolik, 2010; Ginoux et al., 2012). Some studies have noted deficiencies in using individual observation data sets in dust analyses (Tong et al., 2012; Kim et al., 2012), while some others have used AERONET and satellite data sets together to understand the optical properties of dust storm events (Lee et al., 2012). However, the identified physical characteristics and time series of dust storm events vary greatly when based on different data sets. As such, accurate dust climatology and coordinated methods to unify different observational records are still unavailable.

In addition, the influence of meteorological regimes on dust storms is complex, which is also a key issue when studying dust. Dust storms differ in size, duration, and strength, and previous studies on wind erosion have suggested that

the prevailing meteorological conditions play a major role in determining these differences between dust storms (Shao et al., 2002). These characteristics are also helpful for dust storm identification. As pointed out by Shao et al. (2002), the friction velocity, which is determined by the surface wind speed and land surface conditions, is the key factor in regulating dust emission. The strength of dust storms is primarily influenced by the surface wind, resulting from the prevailing weather systems. Therefore, classification of dust storms based on group characteristics and prevailing weather systems is valuable for dust identification and modeling studies.

To improve our understanding of dust storm characteristics and bridge the gaps between different identification methods, we analyze all verified dust storm events reported by the media, previous research, government reports, and the NASA earth observatory over the western US, and then link a series of typical dust storm events through identifiable characteristics gleaned from the application of different data sets. Specifically, we integrate stationary aerosol concentration data from the IMPROVE network, the US EPA AQS data sets, the stationary laser-detected optical information for aerosols provided by the AERONET network, and the AOD observations from the Deep Blue data of MODIS satellites. The differences between these methods are then compared, and the results are linked and assembled in a way that mitigates the deficiencies of using individual data sets. In summation, this study aims to (a) link different data sets in dust storm identification (building communication between physical variables for the same event), (b) find clues as to the meteorological background of dust storms to support future regional dust storm analyses, and (c) suggest new criteria for dust storm identification based on individual data sets.

2 Methodology

The focus in this study is on dust storm events in the past decade, since associated in situ and remote-sensing measurements are comprehensive enough to conduct a better analysis of the identifiable characteristics of dust storms during the period. Due to a lack of specific and consistent recording of dust conditions and activities, we have had to collect dust storm cases over the western US from a variety of sources. These sources include previous published research, federal agency official reports (the United States Geological Survey dust inventory), internet-based media reports, and some significant events recorded by the NASA earth observatory (<http://earthobservatory.nasa.gov>). All events from every source are combined by removing the overlapping counts, based on location and time. Limited by identification method, observational biases, and reporting accuracy, a portion of the events in the combined data set is fake or affected by other sources (e.g., remote dust, anthropogenic dust). Since this study is aimed at collecting characteristics of dust events, we only use events that can be further

confirmed as positive anomalies on either satellite images (MODIS visible or Deep Blue images) or stationary air quality observations (EPA AQS or AERONET). They are then cross-checked with wildfire records from the United States Geological Survey to select reported dust events without influence from wildfire emissions. Events caused by remote dust from Asia or Africa are excluded through the further analysis of satellite records. Finally, a pool of reconfirmed dust storm events is developed, containing 72 reported dust storm events. Since satellite data have daily values and AQS data have hourly values for the recent decade, the effect of data availability on the selection of events is very small. From a statistical point of view, the possible effect may not have any impact on the group characteristics of the random sample.

2.1 Event classification and analysis

We use meteorological observations provided by the National Climatic Data Center (NCDC). The meteorological data set is derived from the integrated surface hourly (ISH) data set (NCDC, 2011). The ISH data set is composed of observations from the Automated Weather Network (AWN), Global Telecommunications System (GTS), and Automated Surface Observing System (ASOS). The meteorological records include basic meteorological factors and a series of codes to describe the weather conditions in a certain hour, which is specific enough to capture rapid or small-scale systems. We first diagnose the weather system that caused the specific dust storm event. Different weather systems are classified into groups (such as cold front, warm front, cyclone, small-scale storm, etc.) by area affected and weather condition. Then we calculate the average surface wind speed (at 10 m height) over the dust storm region during the dust storm hours, which are determined based on hourly ground observations. Other physical variables including temperature, surface air pressure, precipitation type, and wind direction are examined or counted.

With further ensemble diagnostics of weather, satellite, and stationary information on these reported dust storm events, we find that prevailing weather systems can be used for dividing these dust storm events. The dust-impacted area, lasting time, and surface wind speed are diverse under each type of weather system (in Table 2). Based on this diagnosis, dust storms in the western US can be divided into four types using atmospheric conditions: fronts, meso- to small-scale weather systems, disturbances, and cyclogenesis. Fronts, mostly cold, are a kind of rapid weather process that causes strong wind near the ground and blows dust according to the movement of the front. Various meso- to small-scale weather systems in either wet (rain) or dry (little rain) conditions can cause dust storms. For instance, thunderstorms feature strong downward airflow to the ground, which spreads out in all directions, producing strong winds near the surface. Dry meso- to small-scale systems also can create se-

vere dust storms. For example, meso- to small-scale convections along dry lines in Texas usually cause small-scale dust storms. The transportation of atmospheric disturbances from tropical regions is a short-term process that can produce strong surface wind, and it may produce weak dust storms in tropical regions. Cyclogenesis may last several days and can cause strong surface wind during its developing stage (Rauber et al., 2002), which may cause dust emission near the trough. This classification is consistent with characteristics of dust storm size, duration, and strength suggested by previous modeling studies (Shao et al., 2008). Table 1 lists all dust storm events, classified based on their prevailing weather systems. Table 2 provides analyses of meteorological characteristics and pollution properties of reported dust storm events, which further support the classifications in Table 1. The previous study on historical events (Brazel and Nickling, 1986) also supports this classification, based on meteorological evidence.

As shown in Table 1, the most common type of dust storm in the western US is generated by meso- to small-scale weather systems including thunderstorms, convections along dry lines, gusty winds caused by high pressure systems, etc. The most common system is the thunderstorm, in which the organized outflow from the downdrafts of decaying thunderstorms blows dust plumes from source regions. These dust plumes that are blown by the storm then take on the appearance of a moving wall of dust called a haboob, which spans miles and rises thousands of feet into the air. Dust storm events caused by different weather systems show different intensities and identifiable characteristics in observational systems.

In order to build communications among different data sources, we select some typical events as representatives to link physical variables. Previous analyses have focused on the statistical description of group characteristics based on meteorological and air quality measurements. However, limited by data availability, few dust events are fully recorded in all observational systems. To better define identifiable characteristics of dust storms and compare identification methods using different observations, one typical example for each of four dust storm types is selected and analyzed. The sample dust storm cases are selected based on their representativeness and the maximum availability of recording in various data sets. Figure 1 shows the visible, high-resolution satellite images and sketches of the corresponding weather systems for these dust storms. From the images of airborne dust and tracks following weather system movements, qualitative differences in each type of dust storms can be obtained. Clear dust stripes on cloud front events indicate fast and strong emissions. Homogeneous distribution of dust under cyclogenesis shows a relatively slow process. The strong reduction of surface green forest on visible image indicates the high dust concentration in meso-scale events, while the disturbance-caused dust appears as relatively weak signals on visible image. The visible images are influenced by satellite orbits and

Table 1. Classification of reported dust storm events over the western US.

Group	Weather system	Count	Dust storm events (mm/dd/yyyy-state)
1	Fronts	16	12/15/03-TX; 12/22/03-TX; 02/19/04-TX; 05/29/04-KS; 03/16/05-WA; 11/27/05-TX; 10/04/09-WA; 05/03/10-WA; 04/15/11-OK; 10/18/12-KS; 11/10/12-CO-KS; 01/11/13-CO-KS; 08/05/12-OR; 06/04/12-ID; 07/06/09-CO; 10/18/12-NE
2	Meso- or small-scale system	37	04/15/03-TX; 07/23/03-Utah; 08/22/03-AZ; 04/28/04-NV; 04/12/06-AZ; 05/16/06-NV; 06/06/06-AZ; 06/07/06-Utah; 04/28/07-AZ; 07/17/07-AZ; 12/23/07-AZ; 03/14/08-NM; 03/04/09-Utah; 03/07/09-Utah; 04/03/09-AZ; 04/15/09-Utah; 12/30/10-TX; 07/05/11-AZ; 07/07/11-AZ; 07/31/11-AZ; 08/18/11-AZ; 08/26/11-AZ; 02/23/12-Utah; 04/14/12-NM; 04/30/12-TX; 05/09/12-AZ; 06/26/12-AZ; 06/27/12-AZ; 07/21/12-AZ; 07/23/12-AZ; 07/30/12-AZ; 09/06/12-AZ; 01/29/13-NM; 02/09/13-NM; 02/19/13-NM; 08/31/07-ID; 11/04/11-AZ
3	Disturbances	8	11/27/03-CA; 04/18/04-CO; 02/15/06-CA; 03/09/06-CA; 10/04/06-NV; 04/12/07-CA; 04/23/07-NV; 03/18/08-TX
4	Cyclogenesis	11	05/09/04-MN; 01/01/06-TX; 04/06/06-TX; 02/24/07-TX; 01/29/08-TX; 01/22/12-TX; 02/20/12-TX; 03/13/12-WA; 06/25/12-WY; 10/16/12-WY; 03/26/12-WY

dust storm location. Therefore, unlike the qualitative analysis, the quantitative analysis in the following sections is more comprehensive when capturing the characteristics of these typical events.

2.2 Specific analysis in multiple data sets

To better understand the characteristics of dust storm events, we analyze the mass concentrations and optical properties of these events based on the EPA AQS, IMPROVE, and AERONET data sets, as well as the retrieved AOD from the MODIS Deep Blue data set. Among these data sets, only the in situ IMPROVE data have been used previously to identify dust storm activities (Bell et al., 2007; Tong et al., 2012). In comparison, the EPA AQS data set, which has incorporated the aerosol mass observations from the IMPROVE network, has better spatial and temporal coverage for mass concentrations of PM₁₀ and PM_{2.5} (particulate matter with a size less than 10 μm and 2.5 μm, respectively), which is beneficial in mass concentration analysis. Here, the EPA AQS data set and some incorporated PM concentration data from IMPROVE are employed in mass concentration analyses, including examining the statistical properties for each type of dust storm. (<http://www.epa.gov/ttn/airs/airsaqs/detaildata/downloadaqsdata.htm>) Since the increase in aerosol concentrations may be caused by wildfire and/or industrial emissions, we need to check with the United States Geological Survey (USGS) wildfire record and EPA AQS air quality observations to prevent a large amount of noise from influencing the analyses.

Another issue for stationary analyses is the selection of reference sites. In this study, the reference sites are chosen based on the locations of air quality measurements and the availability of observational data (AQS, IMPROVE). We try to find sites near the centers of dust-storm-impacted regions, but in some cases, the sites that best fit the requirements are on the edge of the region affected. The relative location may influence magnitude in mass concentration analyses, though the trend and variability may not seriously be affected. Similar variability also exists in the stationary analyses of optical properties.

The analysis of optical properties focuses on the likelihood of agreement with results from mass concentration analyses of individual dust storm processes. Due to data availability, the optical properties will not extend to the analysis of statistical properties for each type of dust storm. For optical depth observations, the in situ AOD measurements from AERONET are used to study dust storm weather events (Chin et al., 2009; Kim et al., 2011; Lee et al., 2012). Although the AOD measurements from the IMPROVE nephelometer observations have rarely been used, their better temporal resolution may be a good supplement for the missing observations in the AERONET data set. For satellite data, at 550 nm the MODIS Deep Blue data set features AOD observations over land. The available level-3 (L3) data set from the Terra and Aqua satellites has the best temporal and spatial coverage for the western US among satellite products, making it an ideal data set for the identification of dust storms.

For mass concentration analysis, PM₁₀ and PM_{2.5} levels are calculated for each dust storm case, and the ratio of PM_{2.5} to PM₁₀ is examined. These calculations have been

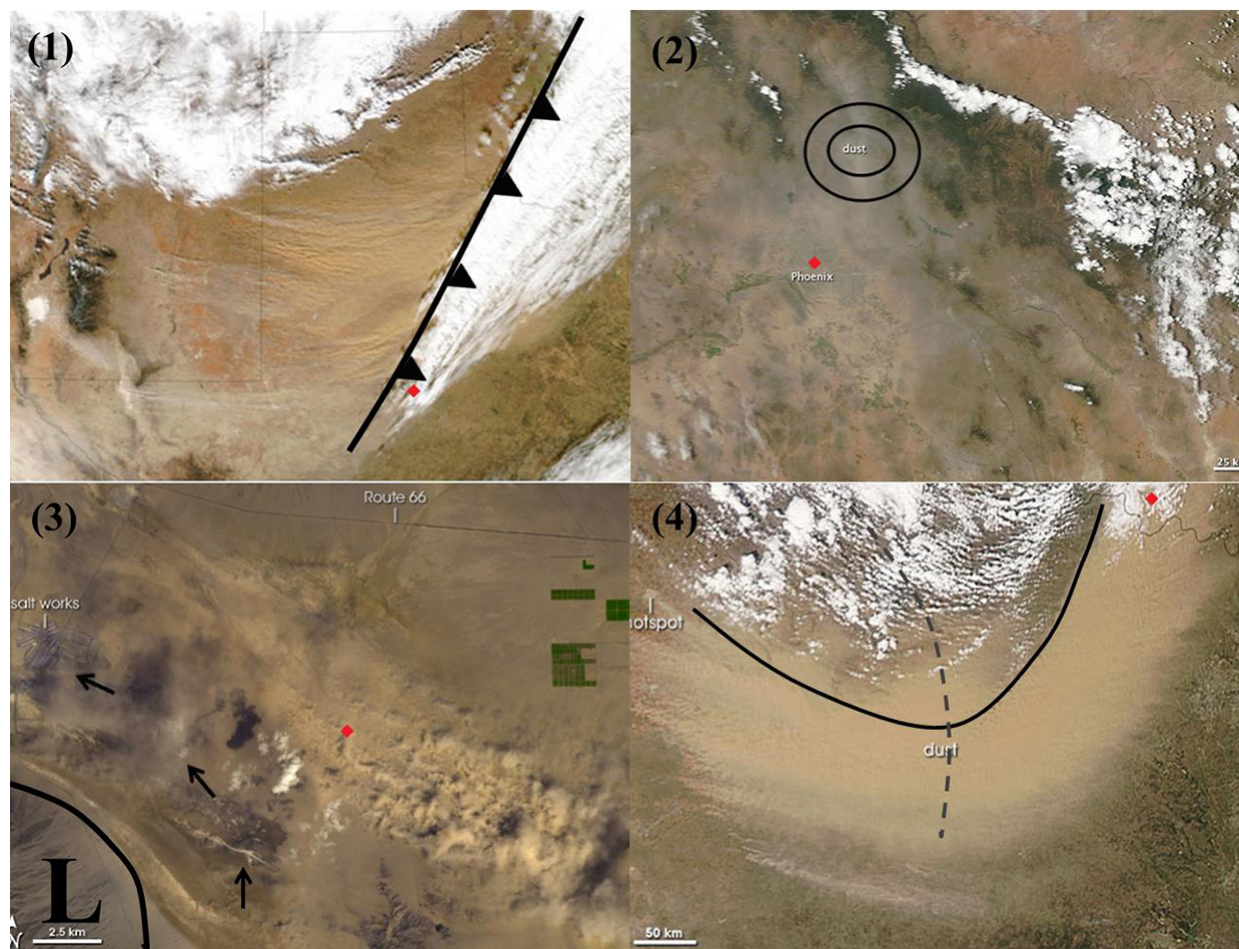


Figure 1. Four typical dust storms over the western United States: visible satellite images and corresponding weather systems for the storms. (1) Dust storm caused by cold front (D1), 15 December 2003, at Texas and Oklahoma border. (2) Dust storm caused by meso- or small-scale system (D2), 5 July 2011, near Phoenix, Arizona. (3) Dust storms caused by disturbances (D3), 12 April 2007, near Amboy, southern California. (4) Dust storm caused by cyclogenesis and associated trough cutoff (D4), 24 February 2007, west of Dallas, Texas. Red marks show the location of available reference air quality sites used in our analyses. (Image credit: NASA earth observatory).

performed in previous dust storm identification studies (Bell et al., 2007; Tong et al., 2012). In this study, however, a group of additional data sets and analyses are employed. These include the following:

1. the ratio of PM_{10} (or $PM_{2.5}$) levels during dust storm hours to the level of PM_{10} (or $PM_{2.5}$) on days without dust storms; the latter are represented by the average of the lowest 80th percentile PM_{10} (or $PM_{2.5}$) concentration recorded in the month and calculated based on AQS hourly PM mass concentration data to understand diurnal variation;
2. the in situ AOD data from the AERONET and IMPROVE nephelometers, which are analyzed to examine the daily and diurnal variability of AOD during the dust storm process;

3. the AOD measurements from the MODIS L3 data set, which are used to determine the strength and spatial impact range of dust storm events; and
4. the statistical information derived from the MODIS data in order to analyze the temporal variation in AOD during dust storm events.

The analyses in multiple data sets explore key characteristics of the sampled dust storms in order to describe the common and specific features of individual types of dust storm events. We pay attention to possible linkages between the mass concentrations and optical properties of these events. Statistical values to describe the group feature of dust storm events are shown (Figs. 2 and 3) as the uncertainty bars over the comprehensive results of typical events for each type. Based on the analyses described above, an improved method is presented for quantifying the characteristics of the typical dust storms selected in this study.

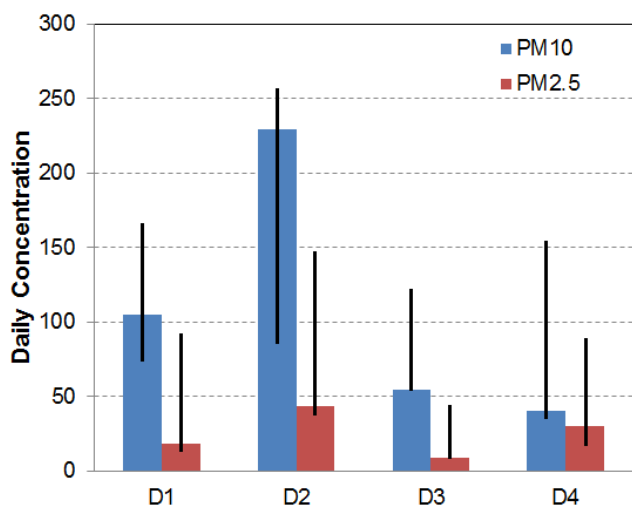


Figure 2. Daily average concentrations of PM₁₀ and PM_{2.5} on dust storm days. Data from sites in dust-storm-impacted regions for four typical events are from the IMPROVE network and the EPA AQS data set. Statistical ranges of ratios for each type are shown by black lines. The analysis is based on the measurements from the AQS site within the dust-storm-impacted area. D1: AQS records for event type 1 (site 480290053 for typical event); D2: AQS records for event type 2 (site PHOE1 for typical event); D3: AQS records for event type 3 (site SAGO1 for typical event); D4: AQS records for event type 4 (site WIMO1 for typical event). (Unit: $\mu\text{g m}^{-3}$.)

3 Results

3.1 Characteristics derived from mass measurements

Mass concentrations of PM are regular variables used in air quality monitoring. In considering the hazardous effects on human health, the National Ambient Air Quality Standards (NAAQS) set the limit for the daily average PM₁₀ level to $150 \mu\text{g m}^{-3}$ and the limit for PM_{2.5} to $35 \mu\text{g m}^{-3}$. Figure 2 shows the daily average concentrations of PM₁₀ and PM_{2.5} at dust-storm-affected sites during these events. With reference to the US EPA NAAQS, the daily averaged concentration of PM₁₀ is above the suggested limit in the case of the dust storms (D2) caused by meso- to small-scale weather systems. The PM_{2.5} level is also above the standard in D2. Previous studies have shown that haboobs caused by strong wind are the most severe dust storms of the four studied types (Brazel, 1986), featuring a rapidly moving dust wall. Cold-front-related dust storms (D1) are also very strong, with a daily average PM₁₀ level above $100 \mu\text{g m}^{-3}$. By contrast, dust storms caused by tropical disturbances (D3) and cyclogenesis (D4) are relatively weak.

From Fig. 2, it is clear that a high PM₁₀ value is a common feature among all types of dust storms. As shown by the black lines, the group features (concentration range) for each type of dust storm event clearly vary and are also similar to the characteristics of their typical event. The differ-

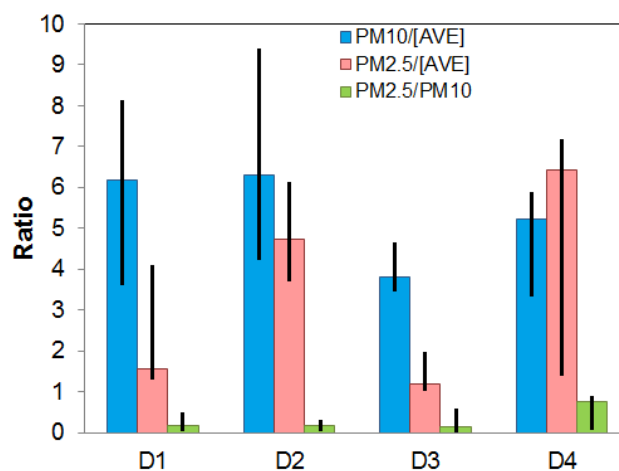


Figure 3. Ratio of PM (PM₁₀ and PM_{2.5}) concentrations on the dust storm days over the lowest 80 % of PM concentrations for the month, and ratio of PM_{2.5} concentration over PM₁₀ on dust storm days. Statistical ranges of ratios for each type are shown by black lines. The analysis is based on the measurements from the AQS site within the dust-storm-impacted area. D1: AQS records for event type 1 (site 480290053 for typical event); D2: AQS records for event type 2 (site PHOE1 for typical event); D3: AQS records for event type 3 (site SAGO1 for typical event); D4: AQS records for event type 4 (site WIMO1 for typical event).

ences in strength among individual events or different groups are mainly affected by the strength of the prevailing weather systems. In addition, the relative location of the observing station with respect to the distribution of dust strength is also an important factor that may affect the strength levels. The erodibility of the land surface in the source region also influences the strength of dust storm events.

Based on daily and hourly PM₁₀ and PM_{2.5} mass concentration records during dust storm events, Fig. 3 illustrates the ratio of PM₁₀ (or PM_{2.5}) levels between dust storm periods and non-dust periods, and also shows the ratio of PM_{2.5} to PM₁₀ during dust storm events. It is evident that the ratio for the PM₁₀ level is between 4 and 7 for the selected typical cases. The ratio for all sample cases studied is between 3 and 10, which indicates a statistic characteristic of dust storm events in affected regions. The same ratio for the PM_{2.5} level is not as uniform. For example, the ratios are high for D2 and D4 and very low for D1 and D3. Reference to USGS wildfire records (<http://wildfire.cr.usgs.gov/firehistory/>), there is a wildfire impact on D2. D4 is located over the industrial region of Texas. Therefore, these differences may be the result of wildfire and industrial emissions, which mainly influence PM_{2.5} concentration levels but have less contribution to PM₁₀ (Urbanski et al., 2009). The relatively low mass concentration of PM_{2.5} could also be a source of uncertainty in computing the ratio of PM_{2.5}. A low mass ratio of PM_{2.5} to PM₁₀ is usually associated with dust storms, as suggested by previous studies (Bell et al., 2007; Tong et al., 2012).

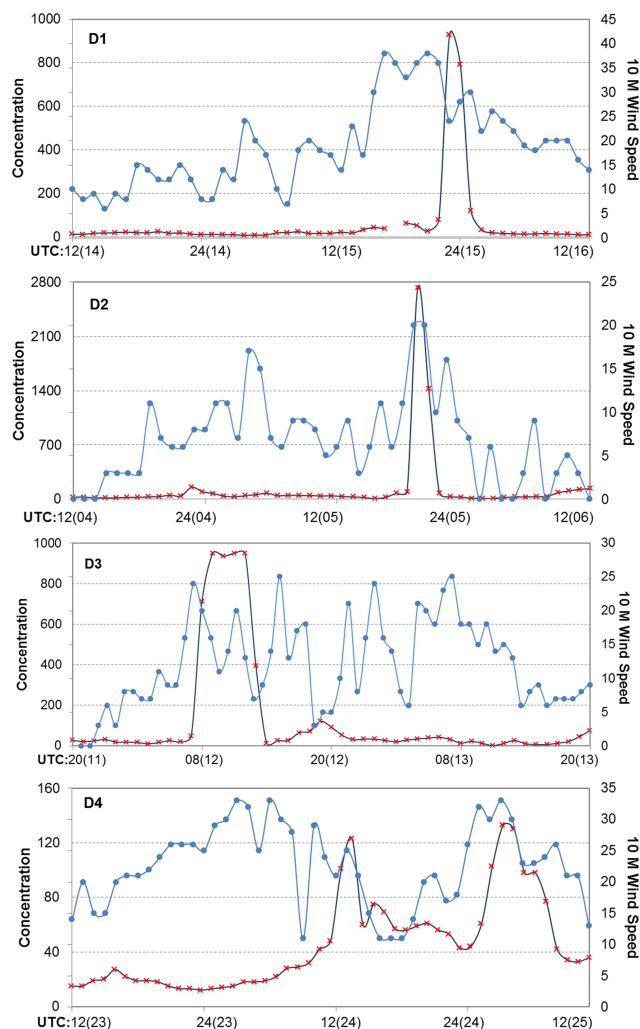


Figure 4. Variations of PM_{10} hourly concentration (unit: $\mu\text{g m}^{-3}$) and surface wind speed at 10 m height (unit: mph) over the dust storm period (48 h surrounding the peak of the dust storm) in the dust-impacted region. Data are from EPA AQS. D1: records on site 480290053 used; D2: records on site 4010 used; D3: records on site 60710306 used; D4: records on site 480290053 used.

However, this ratio may suffer from its intrinsic deficiency as an identification criterion because the ratio for regular days may have already been very low at some sites.

To understand further changes in mass concentration during dust storm events, we analyze the 48 h variation in PM_{10} concentrations around the reported dust storm event. Figure 4 shows the variations in PM_{10} hourly concentrations based on US EPA AQS measurements and local surface wind speed recorded by regular meteorology networks (NCDC, 2011). D1 leads to a sharp increase in PM_{10} to $1000 \mu\text{g m}^{-3}$ in less than 2 hours; however, the high value lasts only for a couple of hours, indicating an intense and fast process. According to the surface wind variation, the dust peak occurs in the strong-wind period. D2 shows similar characteristics, with an even

more powerful and faster dust emission process. Although the wind speed in D2 seems slower than that in the case of D1, surface conditions (soil erodibility, vegetation coverage, etc) also play a crucial role in dust emission. Both D1 and D2 occur in the afternoon, when the boundary layer becomes unstable. D3 occurs in the early morning, when surface winds over land become active, and it lasts for 6 h, with a peak strength of $1000 \mu\text{g m}^{-3}$ according to PM_{10} records. Meteorology data shows that the dust storm event is followed by a precipitation event, which together with the surface wind can well explain the variation of dust storm events. D4 shows dust emission peaks with relatively weak strength in the afternoon and night hours. This may be associated with the relatively slow development of surface instability in cyclogenesis and the diurnal cycle of the boundary layer.

Table 2 summarizes the overall features and meteorological properties of all types of dust storm events. The type of dust storm caused by fronts is very intense and frequently occurs in the central west plain region, as indicated in Table 1. It is associated with high PM_{10} concentrations and strong wind speed, up to 37 m s^{-1} . The affected area featured is very large, from approximately 2×10^4 to $2 \times 10^5 \text{ km}^2$. Dust storms caused by meso- to small-scale weather systems have the fastest process, with a peak PM_{10} concentration up to $3500 \mu\text{g m}^{-3}$. The surface wind is strong, with a speed between 24 and 35 m s^{-1} . However, compared with cold-front-induced dust storms, the areas affected are very limited. Therefore, the dust storms caused by meso- to small-scale systems have the smallest spatial scale. The dust storms caused by tropical disturbances are of medium strength and do not occur very often in our study pool. This type of event usually occurs in California or near the border of the US and Mexico, and it typically lasts 3 to 7 h, with a very limited area affected. It should be noted that dust-impacted areas might also be influenced by terrain and surrounding land use. The dust storms caused by cyclogenesis in middle latitudes are not as strong as the types due to fronts or meso- to small-scale systems. However, they may last up to 21 h and their peak PM_{10} concentration can be very weak, down to $130 \mu\text{g m}^{-3}$. These specific features potentially increase the difficulty of identification.

3.2 Characteristics derived from optical measurements

Owing to the data limitations of optical observations, it is impossible to examine the optical features for all dust storm cases. Since we have examined the group features of all cases in the mass concentration analysis mentioned above, for optical analysis we will focus only on (1) typical cases representing each type, (2) the relationship between the optical feature and mass concentrations, and (3) statistics for optical features in satellite-retrieved AOD for individual cases. Figure 5 shows the variability in AOD from in situ observations during dust storm events. For analysis of optical features, we use the nephelometer-observed AOD values from

Table 2. Statistical and meteorological properties of peak dust storm processes for each type.

Group	Dust storm lasting time range (Hours)	Peak PM ₁₀ range ($\mu\text{g m}^{-3}$)	Size of area affected (km^2)	Wind speed at 10 m (m s^{-1})
Fronts	3–5	431–1765	2×10^4 – 2×10^5	16–37
Meso- or small-scale	2–5	586–3543	5×10^3 – 1.5×10^4	24–35
Disturbances	3–7	476–1137	5×10^2 – 1×10^4	13–26
Cyclogenesis	4–21	137–1392	1×10^4 – 8×10^4	17–29

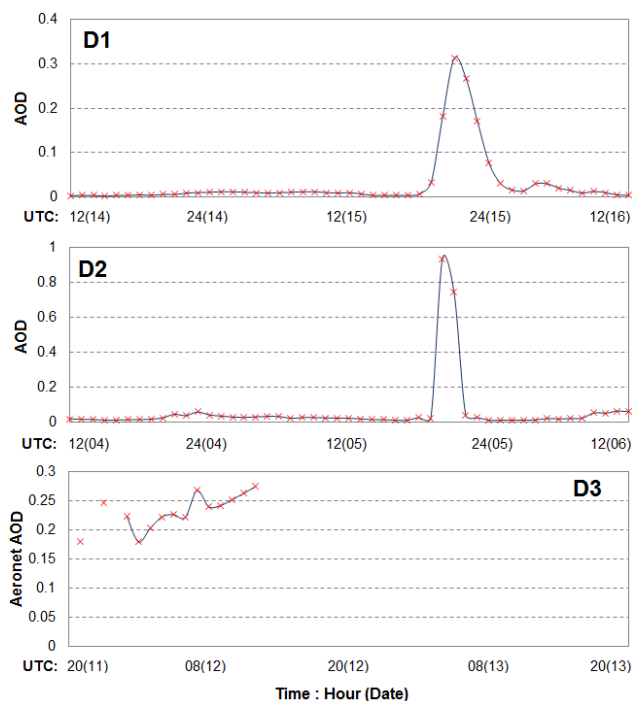


Figure 5. Stationary observations of AOD variation on dust storm day from sites within the dust storm influencing region. D1: from IMPROVE nephelometer (530 nm) monitor on site BIBE1; D2: from IMPROVE nephelometer (530 nm) monitor on site DYRT1; D3: 500 nm AOD from AERONET monitor on site La_Jolla. No stationary AOD measurements available for D4.

the IMPROVE network for D1 and D2 and the AERONET-observed AOD for D3, but no suitable in situ AOD data could be found for D4. As seen in Fig. 5, peaks of AOD concentration last for about 2 hours for both D1 and D2, which is similar to the PM₁₀ results shown in Fig. 4. For D3, the AERONET-observed AOD concentration values during peak hours of dust storms are similar to D1, which is also consistent with the PM₁₀ concentrations. These results suggest that the IMPROVE nephelometer 530 nm AOD is comparable to the AERONET 500 nm AOD, which is in agreement with previous studies (reference: http://alg.umbc.edu/neph/Neph_AOT.html).

Satellite-retrieved AOD concentrations on specific dust storm days are added to the analysis of events. Figure 6 shows the daily mean AOD distribution over land from the MODIS Deep Blue (550 nm) data for the selected examples. Significant changes in aerosol optical depth over the western United States may be attributable to dust emissions, wildfires, and severe air pollution episodes. Wildfire records from USGS are used to preclude the contribution from wildfires. Based on AQS pollution records, anthropogenic air pollution episodes are not found in these example cases. For D1, the high AOD values are near the border of Texas and New Mexico, circled by a solid line, which captures the area impacted by the dust storm event. Caution must be exercised when using satellite images to identify dust events, as not all high MODIS AOD values represent dust storm events. Wildfires may also contribute to high AOD in satellite images. For example, in D2, it is noted that two regions feature high AOD values: one over Arizona circled by a solid line, and the other circled by a dashed line over a broader area across the borders of New Mexico, Texas, Colorado, and Oklahoma. By cross-checking with wildfire records from 2011, it is easy to determine that the latter was caused by the Las Conchas wildfire, which started on 26 June 2011 and lasted over a month. Additionally, the scattered high values of MODIS AOD over California correspond to the dust storm on 5 July 2011, captured by local, in situ records. For D3, major characteristics of the event are high AOD values over southern California. If using MODIS data alone, other possible dust storms may be identifiable in Nevada and eastern Kansas; however, they are not validated by stationary observations. For D4, the highest values of MODIS AOD are over the area of Texas circled on the map, and another weaker event is near the border between California and Arizona.

Previous analyses have shown that satellite images can provide important information for the identification of dust storms, though contaminated signals may result because of other environmental events. More importantly, satellite-retrieved AOD can provide useful information on dust-storm-affected areas and on the spatial extent of dust storm strength. It is clear that cold-front-related dust storms have a large affected region, while meso- to small-scale systems cause dust storms to have greater strength. It should be noted that satellite information is affected and limited by the satellite's

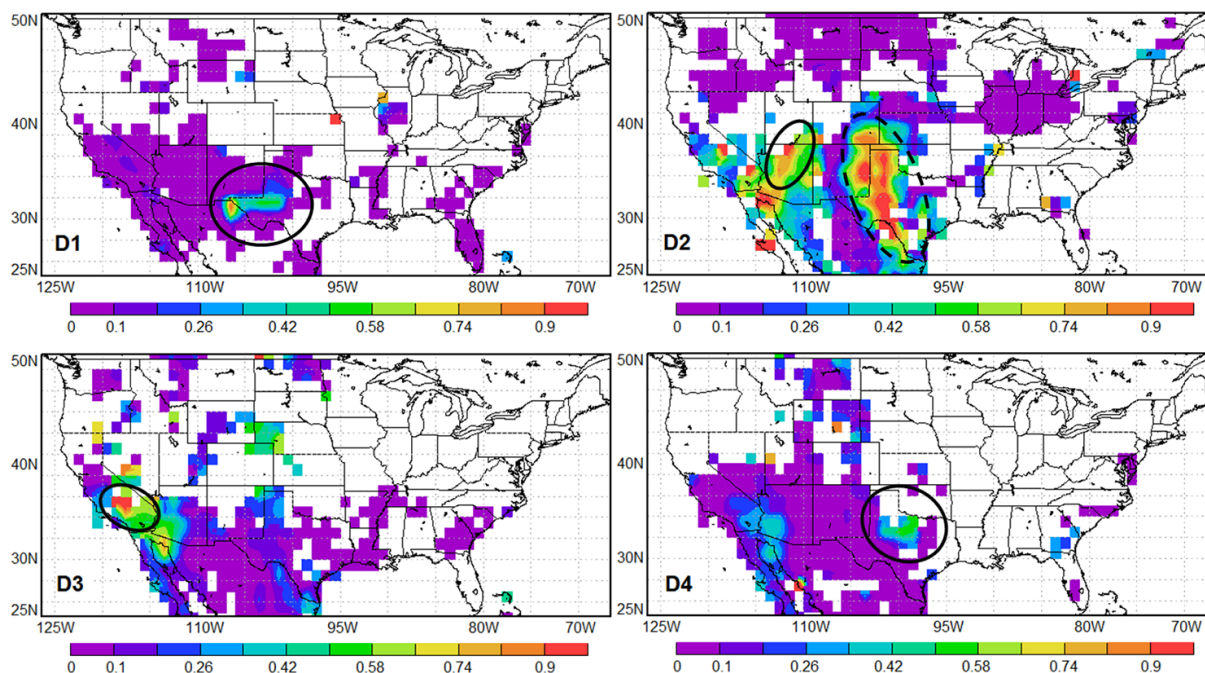


Figure 6. Mean aerosol optical depth over land using MODIS Deep Blue (550 nm) data. The result is based on the level-3 products for the dust storm day (from the combined data set of Terra and Aqua). Regions circled by solid lines are dust storm regions. Regions circled by dashed lines are wildfire regions according to the wildfire record. (D1: 15 December 2003; D2: 5 July 2011; D3: 12 April 2007; D4: 24 February 2007.)

swath coverage and frequency. For example, satellite images may miss certain rapid and small-scale dust storm processes. Therefore, we need to use the statistics computed from the satellite AOD values to capture more information and achieve a better understanding of the processes. The basic method is to statistically analyze all the on-grid AOD values within the dust storm area and period. Based on statistic properties, more comprehensive information about the dust storm process can be extended.

Figure 7 shows the satellite data retrieved to examine the variability in AOD during the dust storm process. The bar chart presents the values of the mean, maximum, minimum, and standard deviation of daily satellite AOD for each dust event. The mean values of MODIS AOD are comparable in magnitude to those of the in situ observations of AOD, which may partially be because the latest version of the MODIS AOD data set was calibrated with the in situ observations (Lee et al., 2012). The only difference is that the satellite value represents a spatial average, while the in situ observation is for a specific location. Therefore, the stationary AOD and concentration measurements should be associated with a satellite AOD value between the maximum and minimum. Figure 7 also shows that D1 has the largest variability in satellite AOD records. However, dust emission may be distributed unevenly within an area and thus can cause a large standard deviation, which can be a good indicator for dust storm identification. D2 shows a high mean value of AOD

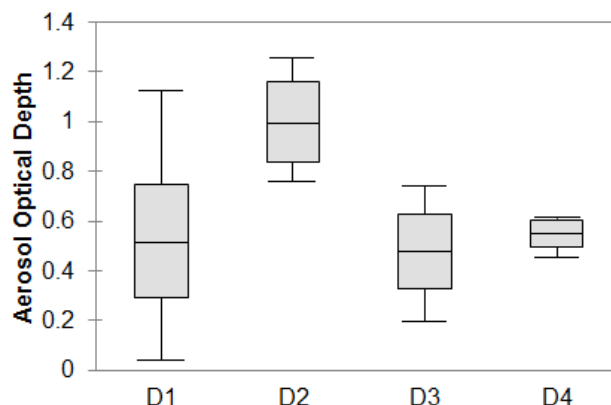


Figure 7. Statistical characteristics of aerosol optical depth variation in MODIS Deep Blue (550 nm) data set during four dust storm days (from the combined data set of Terra and Aqua). The top bar shows the maximum AOD of the day recorded by satellite; the bottom bar shows the minimum AOD of the day recorded by satellite; the bar in the rectangle shows the mean AOD value of all satellite records during the day; top and bottom edges of the rectangle show the values one standard deviation away from the mean AOD.

with low variability, which indicates that the effect of D2 on air quality is stronger and broader. Compared with D3, which has a similar mean value, D4 shows the least variability in the AOD records. This feature indicates that dust concentration

within the examined grid is rather uniform, which accords with the analysis of mass concentrations.

4 Discussion and conclusion

In order to improve dust storm identification over the western United States, a collection of dust storm events measured by air quality and satellite observations is analyzed based on characteristics in meteorological data, satellite aerosol optical depth (AOD) retrievals, and air quality data sets. Stemming from the prevailing weather systems and their associated physical conditions related to dust emission, dust storm events are classified into four typical types. We find that the typical characteristic of front-induced dust storms is a rapid process with strong dust emissions and large affected area. Dust storms caused by rapid meso- to small-scale systems are the strongest, with a rapid process producing the highest levels of dust emissions in a limited area. Dust storms due to disturbances show strong air concentrations of dust and last longer than the events due to cold fronts and meso- to small-scale systems. Cyclogenesis-induced dust events are the longest-lasting storms, since the cyclogenesis tends to be stationary. Statistical analyses of the spatial and temporal characteristics of dust storm events of each type show significant diversity.

These four types of dust storm events are sampled and examined to explore their identifiable characteristics based on in situ and remote-sensing measurements. Generally, we find that these data sets are capable of describing and differentiating dust storm processes. The analysis of mass concentration measurements shows that hourly AQS records are able to reveal details of the mass concentration changes of dust storm processes. The analysis also indicates that the relative ratio of PM_{10} between levels during the dust storm day and the mean level may be a better indicator of dust storm events than that provided by the in situ mass observation data sets. Our analysis also shows that this ratio is high for all types of dust storms, irrespective of the large differences in the strength of the events. Stationary aerosol optical property measurements can identify the differences between types of dust storm events. Besides the AOD characteristics, satellite data provide specific information about dust-storm-affected areas and the strength distribution. We find that the statistical properties of AOD provided by satellite data sets also provide information for delineating the dust storm process. In addition, this study also suggests that wildfire emissions are a significant source of noise in dust storm identification using the MODIS AOD data set, and that they can be filtered out based on existing archives of wildfire records.

With the analyses described above, we compare the characteristics of typical dust events shown in different data sets in order to determine the identification criteria of dust storm events. The results have shown that the variability in mass concentrations during dust storm processes captured only by

in situ observations is consistent with the variability in AOD from stationary or satellite observations. The peak AOD observed on the ground is consistent with satellite AOD measurements. MODIS-retrieved AOD from the Deep Blue algorithm can capture the dust strength variation during a dust storm process. In conclusion, we find that the combination of different data sets is a better approach for capturing common characteristics of a type of dust storm and for providing specific information about a particular event. Specifically, the meteorological data are good at identifying the lasting period and area impacted by a dust event. The ground-based air quality and optical measurements capture the peak strength well. Moreover, aerosol optical depth from satellite data sets allows us to better identify dust-storm-affected areas and the spatial extent of dust. The study also suggests that the combination of in situ and satellite observations would be a better method to fill gaps in dust storm recordings.

Acknowledgements. This series of studies is supported by NASA National Climate Indicator Project (12-INCA12-0056). We appreciate further discussions of U.S. dust storms with Daniel Tong, Paul Ginoux, and Thomas Gill.

Edited by: X. Liu

References

- Baddock, M. C., Bullard, J. E., and Bryant, R. G.: Dust source identification using MODIS: a comparison of techniques applied to the Lake Eyre Basin, Australia, *Remote Sens. Environ.*, 113, 1511–1528, 2009.
- Bell, M. L., Dominici, F., Ebisu, K., Zeger, S. L., and Samet, J. M.: Spatial and temporal variation in $PM_{2.5}$ chemical composition in the United States for health effects studies, *Environ. Health Persp.*, 115, 989–995, 2007.
- Brazel, A. J. and Nickling, W. G.: The relationship of weather types to dust storm generation in Arizona (1965–1980), *J. Climatol.*, 6, 255–275, 1986.
- Chin, M., Diehl, T., Dubovik, O., Eck, T. F., Holben, B. N., Sinyuk, A., and Streets, D. G.: Light absorption by pollution, dust, and biomass burning aerosols: a global model study and evaluation with AERONET measurements, *Ann. Geophys.*, 27, 3439–3464, doi:10.5194/angeo-27-3439-2009, 2009.
- Ginoux, P., Prospero, J. M., Gill, T. E., Hsu, N. C., and Zhao, M.: Global-scale attribution of anthropogenic and natural dust sources and their emission rates based on MODIS deep blue aerosol products, *Rev. Geophys.*, 50, RG3005, doi:10.1029/2012RG000388, 2012.
- Hahnenberger, M. and Nicoll, K.: Meteorological characteristics of dust storm events in the eastern Great Basin of Utah, USA, *Atmos. Environ.*, 60, 601–612, doi:10.1016/j.atmosenv.2012.06.029, 2012.
- Holben, B. N., Eck, T. F., Slutsker, I., Tanre, D., Buis, J. P., Setzer, A., Vermote, E., Reagan, J. A., Kaufman, Y. J., Nakajima, T., Lavenu, F., Jankowiak, I., and Smirnov, A.: AERONET – A

- federated instrument network and data archive for aerosol characterization, *Remote Sens. Environ.*, 66, 1–16, 1998.
- Kahn, R. A., Nelson, D. L., Garay, M. J., Levy, R. C., Bull, M. A., Diner, D. J., Martonchik, J. V., Paradise, S. R., Hansen, E. G., and Remer, L. A.: MISR aerosol product attributes and statistical comparisons with MODIS, *IEEE T. Geosci. Remote*, 47, 4095–4114, doi:10.1109/TGRS.2009.2023115, 2009.
- Kim, D., Chin, M., Yu, H., Eck, T. F., Sinyuk, A., Smirnov, A., and Holben, B. N.: Dust optical properties over North Africa and Arabian Peninsula derived from the AERONET dataset, *Atmos. Chem. Phys.*, 11, 10733–10741, doi:10.5194/acp-11-10733-2011, 2011.
- Kim, D., Chin, M., Bian, H., Tan, Q., Brown, M. E., Zheng, T., You, R., Diehl, T., Ginoux, P., and Kucsera, T.: The effect of the dynamic surface bareness to dust source function, emission, and distribution, *J. Geophys. Res.*, 118, 1–16, doi:10.1029/2012JD017907, 2012.
- Lee, J., Kim, J., Yang, P., and Hsu, N. C.: Improvement of aerosol optical depth retrieval from MODIS spectral reflectance over the global ocean using new aerosol models archived from AERONET inversion data and tri-axial ellipsoidal dust database, *Atmos. Chem. Phys.*, 12, 7087–7102, doi:10.5194/acp-12-7087-2012, 2012.
- Lei, H., Lin, Z., and Sun, J.: An improved dust storm prediction system and its simulation experiments, *Clim. Environ. Res.*, 10, 669–683, 2005.
- Lin, Z., Levy, J., Lei, H., and Bell, M.: Advances in Disaster Modeling, Simulation and Visualization for Sandstorm Risk Management in North China, *Remote Sens.*, 4, 1337–1354, 2012.
- Prasad, A. K. and Singh, R. P.: Changes in aerosol parameters during major dust storm events (2001–2005) over the Indo-Gangetic Plains using AERONET and MODIS data, *J. Geophys. Res.-Atmos.*, 112, D09208, doi:10.1029/2006JD007778, 2007.
- Prospero, J. M.: Long-term measurements of the transport of African mineral dust to the southeastern United States: implications for regional air quality, *J. Geophys. Res.*, 104, 15917–15927, 1999.
- Rauber, R. M., Walsh, J., and Charlevoix, D.: *Severe and Hazardous Weather*, Kendall Hunt Publishing Company, Dubuque, IA, USA, 616 pp., 2002.
- Remer, L. A., Kaufman, Y. J., Tanre, D., Matoo, S., Chu, D. A., Martins, J. V., Li, R.-R., Ichoku, C., Levy, R. C., Kieidman, R. G., Eck, T. F., Vermote, E., and Holben, B. N.: The MODIS aerosol algorithm, products, and validation, *J. Atmos. Sci.*, 62, 947–973, doi:10.1175/JAS3385.1, 2005.
- Schubert, S. D., Suarez, M. J., Pegion, P. J., Koster, R. D., and Bacmeister, J. T.: On the cause of the 1930s dust bowl, *Science*, 303, 1855–1859, 2004.
- Shao, Y., Jung, E., and Leslie, L. M.: Numerical prediction of northeast Asian dust storms using an integrated wind erosion modeling system, *J. Geophys. Res.*, 107, 4814, doi:10.1029/2001JD001493, 2002.
- Tanaka, T. Y. and Chiba, M.: A numerical study of the contributions of dust source regions to the global dust budget, *Global Planet. Change*, 52, 88e104, doi:10.1016/j.gloplacha.2006.02.002, 2006.
- Tong, D. Q., Dan, M., Wang, T., and Lee, P.: Long-term dust climatology in the western United States reconstructed from routine aerosol ground monitoring, *Atmos. Chem. Phys.*, 12, 5189–5205, doi:10.5194/acp-12-5189-2012, 2012.
- Torres, O., Bhartia, P. K., Herman, J. R., Sinyuk, A., Ginoux, P., and Holben, B.: A long-term record of aerosol optical depth from TOMS observations and comparison to AERONET measurements, *J. Atmos. Sci.*, 59, 398–413, 2002.
- Urbanski, S. P., Hao, W. M., and Baker, S.: *Chemical Composition of Wildland Fire Emissions, Developments in Environmental Science*, 8, 79–107, ISSN:1474-8177/10.1016, 2009.
- Waggoner, D. G. and Sokolik, I. N.: Seasonal dynamics and regional features of MODIS-derived land surface characteristics in dust source regions of East Asia, *Remote Sens. Environ.*, 114, 2126–2136, 2010.
- Woodward, S.: Modeling the atmospheric life cycle and radiative impact of mineral dust in the Hadley Centre climate model. *J. Geophys. Res.*, 106, 18155–18166, doi:10.1029/2000JD900795, 2001.
- Zhao, C., Liu, X., and Leung, L. R.: Impact of the desert dust on the summer monsoon system over southwestern North America, *Atmos. Chem. Phys.*, 12, 3717–3731, doi:10.5194/acp-12-3717-2012, 2012.